African Journal of Advanced Pure and Applied Sciences (AJAPAS)

Online ISSN: 2957-644X

Volume 2, Issue 2, April-June 2023, Page No: 137-147

Website: *https://aaasjournals.com/index.php/ajapas/index*

||Arab Impact factor 2022: 0.87|| SJIFactor 2022: 4.308 || ISI 2022: 0.557

Modelling the Optical Band Gap Energy of Undoped ZnO Thin Films by Supervised Machine Learning Methods

Maryam Akhwater [*]

Department of physics, Faculty of art and science – Almarj, University of Benghazi, Libya.

[*]*Corresponding author: marymuhammed14@gmail.com*

Received: March 11, 2023	Accepted: April 20, 2023	Published: May 06, 2023

Abstract:

Recently, machine learning (ML) methods are growing as one of the most powerful techniques in scientific research and technological applications. Herein, artificial neural networks (ANNs) as novel predictive ML techniques were built to predict the optical band gap energy of undoped ZnO thin films. The proposed multilayer perceptron neural network methods include the scaled conjugate gradient (SCG) and the gradient descent (GD) with momentum and learning rate optimization coefficients.

The two suggested techniques were trained, tested, and validated with empirical data sets, by selecting the temperature of the substrate and the precursor molarity of ZnO solution as input parameters as well as the band gap energy as a response parameter. Furthermore, the simulated findings of ANN models were compared to the multiple linear regression (MLR) model and then the fitness and accuracy of those models were evaluated by different statistical metrics including the root mean square error (RMSE), the mean absolute percentage error (MAPE), and regression coefficients. Based on the results, SCG-ANN and GD-ANN models show high prediction accuracy with RMSE of 0.055 and 0.064 for testing data, respectively, whilst MLR analysis showed poor prediction accuracy with RMSE of 0.080 and R^2 of 0.063. Additionally, the simulated output of these proposed ANNs models is in good agreement with the empirical datasets, which indicates high performance of SCG-ANN and GD-ANN models than the MLR model.

Keywords: Machine Learning, Undoped ZnO, Band Gap, Energy, Neural Networks.

Cite this article as: M. Akhwater, "Modelling the Optical Band Gap Energy of Undoped ZnO Thin Films by Supervised Machine Learning Methods," *African Journal of Advanced Pure and Applied Sciences (AJAPAS)*, vo2. 1, no. 2, pp. 137–147, April-June 2023.

Introduction

Recently, zinc oxide (ZnO) nanostructures have gained great attraction as a superior material for developing high performing ZnO-based devices and applications. However, it is challenging to characterize the synthesis process of ZnO thin films due to the nonlinearity nature and unpredictability changes during the fabrication process. Hence, for highly efficient optical devices the correlations among the different input and output parameters of the synthesis process have to be investigated statistically. Therefore, generating a sophisticated mathematical model which forecasts and optimizes the nonlinear features of those nanostructures can significantly improve their performance. In material science, the luminescence yield of direct band gap materials is higher than those of indirect band gap materials which means the direct wide band gap energy lowers the leakage current of the systems and their temperature-dependent properties [1]. ZnO has a direct large band gap energy (3.40 eV) at room temperature that makes it transparent in the visible light region and highly photoactive in the UV region. Furthermore, ZnO has Higher exciton binding energy (~60 m eV) which can increase its

photo-activity and make it an attractive material for short wavelength optoelectronic devices [2]. In addition, the high exciton binding energy in ZnO materials can enhance (UV) luminescence (~380 nm) at room temperature [3]. Based on the photoluminescence (PL) spectroscopy of ZnO nanorods, it was observed that the quantum confinement effect is generally related to the small sizes of ZnO grains and can result in increasing the band gap energy and exciton binding energy [4]. A strong luminescence peak at 380 nm was attributed to band-to-band transitions and green-yellow emission was observed due to oxygen vacancy. Another red emission peak was also reported, which is explained as transitions caused by a doubly ionized oxygen vacancy [5]. Further, as ZnO nanowire/nanorod has a nearly cylindrical shape and large refractive index (~2.0), therefore, it is an attractive material for optical waveguides [6].

In data science, ML is a branch of artificial intelligence applications, where ML algorithms inspire or simulate to mimic the human brain. Those ML algorithms are considered as a powerful informatic method to process data, which is mostly available through previously published reviews, for learning and predicting the desired results. Hence, ML can significantly speed up the manufacturing process of nanostructures-based devices and applications without employing multiple repeated estimations [7]. One of the most used ML methods is ANNs which is applied for forecasting different material properties and producing the optimum parameters of the manufacturing process.

ANN was combined with an adaptive network-based fuzzy inference system (ANFIS) to predict the antibacterial growth of knitted fabrics. Based on the findings, high performance with good efficiency was verified for both models [8]. Another study developed ANN and golden eagle optimizer (GEO) to assess the comfort characteristics of zinc oxide nanoparticles (ZnO NPs) coated woven fabrics. It found that the ANN-GEO model offers better accuracy compared to the standard ANN model [9]. In addition, the tensile strength of wool fibres was predicted by employing ANN with multiple linear regression, according to the results, the ANN approach was more efficient and accurate than multiple linear regression [10]. In another work, ANN, and Kernel Ridge Regression (KRR) were used to forecast the band gap energy of ZnO quantum dots. The models result showed significant accuracy and good performance [11]. Further, The Levenberg-Marquardt (LM) algorithm of ANN was employed to forecast the crystallite size and band gap energy of ZnO quantum dots. According to the results, the model had a high prediction accuracy [12].
In the current study, the aim is to apply different predictive algorithms, namely, SCG-ANN, GD-ANN, and MLR model to predict the band gap energy of undoped ZnO thin films. Moreover, the efficiency and accuracy of those models were validated as an anticipation technique through analytical methodology, and the relationship between the input variables and the response factor was proved.

ANNs modelling methodology

Herein, an applied strategy is to identify the best anticipating algorithms which can produce the most optimum output response through several groups of input factors. The basic principles of ANN are to imitate the nature and performance of the biological neurons of the human brain that enable those artificial networks to determine the linear and nonlinear interconnections among the dependent and independent parameters. A fundamental unit of ANN is an artificial neuron (node), which has a layered structure and can supervise the input and deliver the output to other neurons in a network. Initially, when an artificial neuron receives the input that is weighted, it decides whether the output signal should be feedforward to the following layer as input. Such a decision-making process is known as bias, and it is defined via the activation function built into the network system [13].

In multilayer perceptron ANN the data is feedforwarded from input to output neurons in one direction with no back loops through several hidden layers. It can also minimize the gradient error by adjusting weight and biases in non-linear models [13]. Herein, the designed multilayer perceptron ANNs start by initializing the weights and threshold values and setting the hyperparameters and then, training the model by propagating forward the inputs layer by layer to generate the output response. When the error gradient is evaluated, it would be propagated backwards, and the weights and biases would be updated (see Fig. 1).

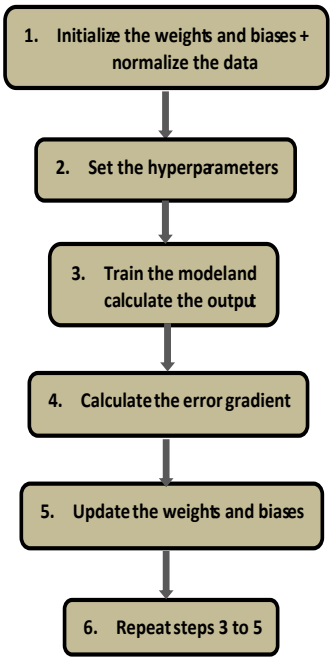

Fig. 1: A schematic diagram of the optimization process of ANN algorithms.

In general, the output of the dependent variable (y) is predicted for a group of the input of independent variables (x) as shown in Eq. (1) [9].

$$y = f\sum_i w_i * x_i + b \qquad (1)$$

Where y is the network output, x_i describes the input values, w_i describes the weights, b is the biases, and f is the activation function. The basic structure of feedforward ANNs in the current study contains four layers which are one input layer, one output layer and two hidden layers (see Fig. 2). The objective is to build different predictive approaches based on ANN algorithms and classical MLR model using the experimental data sets of undoped ZnO thin films, which were obtained from international journals [14-40].

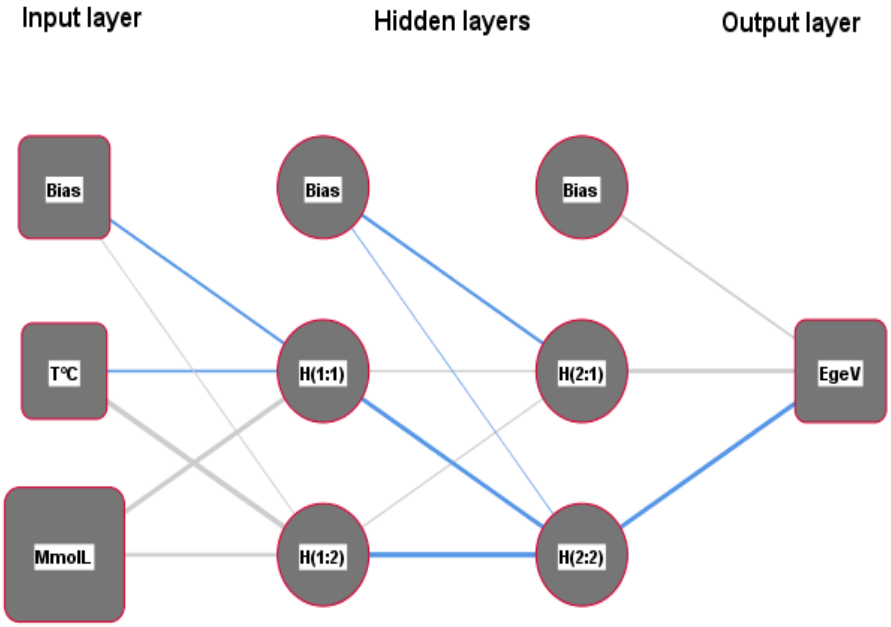

Fig. 2: A basic diagram of ANN models.

The ANN- SCG and ANN- GD models were built and tested using the Neural Network Toolbox from IBM SPSS software version 26. Two input parameters namely, the substrate temperature and the solution concentration were investigated with regard to the band gap energy as the output response. The datasets were partitioned to be trained, tested, and validated. The training data was used to identify the weights and build the model, while the testing data was employed to determine errors and prevent overtraining during the training stage. To evaluate the model accuracy, the band gap energy was predicted with the independent factors in the test dataset and then the results were compared with the targeted values of the band gap energy in the test dataset. In addition, the Prediction performance of the ANN- SCG and ANN- GD models was compared to the MLR model

Results and discussion

In general, the ANNs performance is considerably influenced by the type of proposed algorithms, the number of hidden layers, the hyperparameters of the training process, and the activation functions which can lead to generating a high performing model by optimizing the neural network output. In the current work, two supervised learning ANNs algorithms were applied with the mostly used nonlinear activation functions, namely sigmoid and hyperbolic tangent functions. To identify the most efficient models, the hyperbolic tangent and sigmoid functions were employed as input and output functions respectively, in models ANN- SCG (1) and ANN- GD (1) respectively. Whilst models ANN- SCG (2) and ANN- GD (2) were trained by applying the sigmoid and hyperbolic tangent functions as input and output activation functions, respectively. All ANN- GD models were trained with learning rates of 0.2 and momentum parameters of 0.75. furthermore, a classical MLR analysis was utilized as a predictive technique to evaluate the band gap energy of undoped ZnO thin films, and each model was trained by the empirical data sets which are summarized in table (1).

Table. 1 the input experimental data sets of undoped ZnO thin films.

T (°C)	M (mol/L)	Eg (eV)	Ref
350	0.05	3.08	14
350	0.075	3.22	14
350	0.1	3.37	14
350	0.125	3.15	14
350	0.1	3.1	15
450	0.05	3.25	16
300	0.1	3.06	17
350	0.02	3.19	18
300	0.1	3.168	19
350	0.1	3.25	19
400	0.1	3.229	19
200	0.1	3.31	20
350	0.1	3.27	20
500	0.1	3.28	20
300	0.1	3.292	21
350	0.1	3.317	21
400	0.1	3.441	21
350	0.1	3.27	22
450	0.2	3.29	23
410	0.1	3.26	24
350	0.1	3.42	25
350	0.1	3.304	26
300	0.1	3.25	27
200	0.1	3.4	28
250	0.1	3.15	29
300	0.1	3.222	29
350	0.1	3.25	29
400	0.1	3.275	29
450	0.1	3.275	29
285	0.2	3.28	30

450	0.2	3.285	31
450	0.05	3.25	32
450	0.1	3.277	33
450	0.05	3.29	34
400	0.1	3.125	35
460	0.01	3.28	36
375	0.1	3.24	37
450	0.2	3.37	38
450	0.1	3.28	39
400	0.1	3.29	40

The forecasting performance and accuracy for the designed ANN models were determined via different statistical metrics, including RMSE (Eq. (2)), MAPE (Eq. (3)), the R^2 coefficient (Eq. (4)), and the relative error (r) (Eq. (5)).

$$RMSE = \sqrt{\frac{1}{n}\sum_{i=1}^{n}(y_t - y_t^{i})^2} \quad (2)$$

$$MAPE = \frac{1}{n}\sum_{i=1}^{n}\frac{\left|y_t - y_t^{i}\right|}{y_t} * 100 \quad (3)$$

$$R^2 = 1 - \sum_{i=1}^{n}(y_t - y_t')^2 \Big/ \sum_{i=1}^{n}(y_t')^2 \quad (4)$$

$$r = \frac{Sim_{out} - Act_{out}}{Act_{out}} \times 100 \quad (5)$$

Where y_t, and y'_t are the observed and targeted band gap energy values respectively, and n is the total number of datasets. The mathematical metric error RMSE is used to assess the model performance; it has always a positive value and the optimum case should be zero. The RMSE values for all proposed models are summarized in Table. 2.

Table. 2. The statistical metrics errors of the proposed ANNs and MLR models**.**

Model	RMSE (training)	RMSE (testing)	MAPE %	R^2	r
ANN- GD (1)	0.121	0.055	1.70	0.9999	0.969
ANN- SCG (1)	0.127	0.064	1.71	0.9993	0.979
ANN- GD (2)	0.240	0.125	1.73	0.9988	1.163
ANN- SCG (2)	0.212	0.195	1.75	0.9983	1.186
MLR	RMSE=0.080			0.063	

Lower values of RMSE refer to the high performance of the suggested algorithms, as can be noticed from Table 2. When all models were trained, ANN-GD (1) and ANN-SCG (1) were the most ideal ones with RMSE of 0.055 and 0.064 for testing data, respectively. In addition, the R^2 coefficient shows how precise the simulated values of models near fit or fit the targeted values, and favourably the highest value refers to the well-fitted model with a strong correlation among the simulated and targeted data. The performance of the suggested ANNs models in terms of the R^2 coefficient is shown in Table 2. The ANN-GD (1) and ANN-SCG (1) displayed the

best fit by the obtained results of 0.9999 and 0.9993 than the classical MLR model. Moreover, it observed that ANN-GD (1) and ANN-SCG (1) models had a lower relative error of 0.969 and 0.979 respectively. Therefore, the most creditable models according to evaluated output were ANNs models, whilst the MLR model emphasized lower prediction accuracy in terms of RMSE of 0.080 and R^2 of 0.063.

Additionally, it found based on a comparison of simulated and targeted network output of band gap energy for the validated ANN-GD (1) and ANN-SCG (1), satisfactory performance and high efficiency of those models shown in Figs. 3, 4.

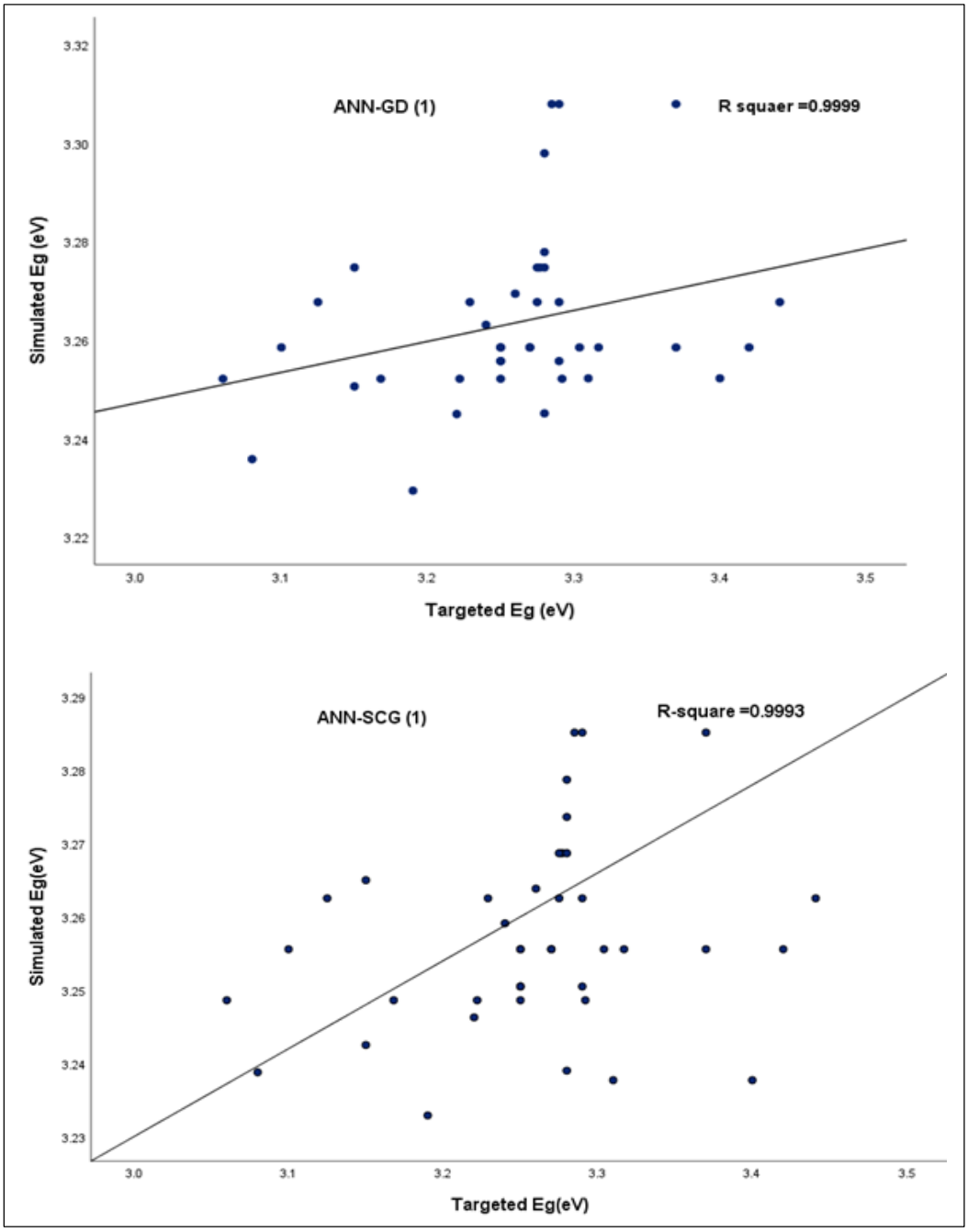

Fig. 3. Scatter plots of ANN-GD (1) and ANN-SCG (1) for simulated and targeted values.

Points located on or nearby the line have an ideal prediction than those that are away from the line, also there are no obvious patterns. The regression plots showed an 'excellent fit' proving that the network output of proposed ANNs models was approximately similar to the empirical output. Moreover, it essential to plot residuals versus fitted data, since the residuals are an indicator to the differences between measured and simulated data of the assumed models.

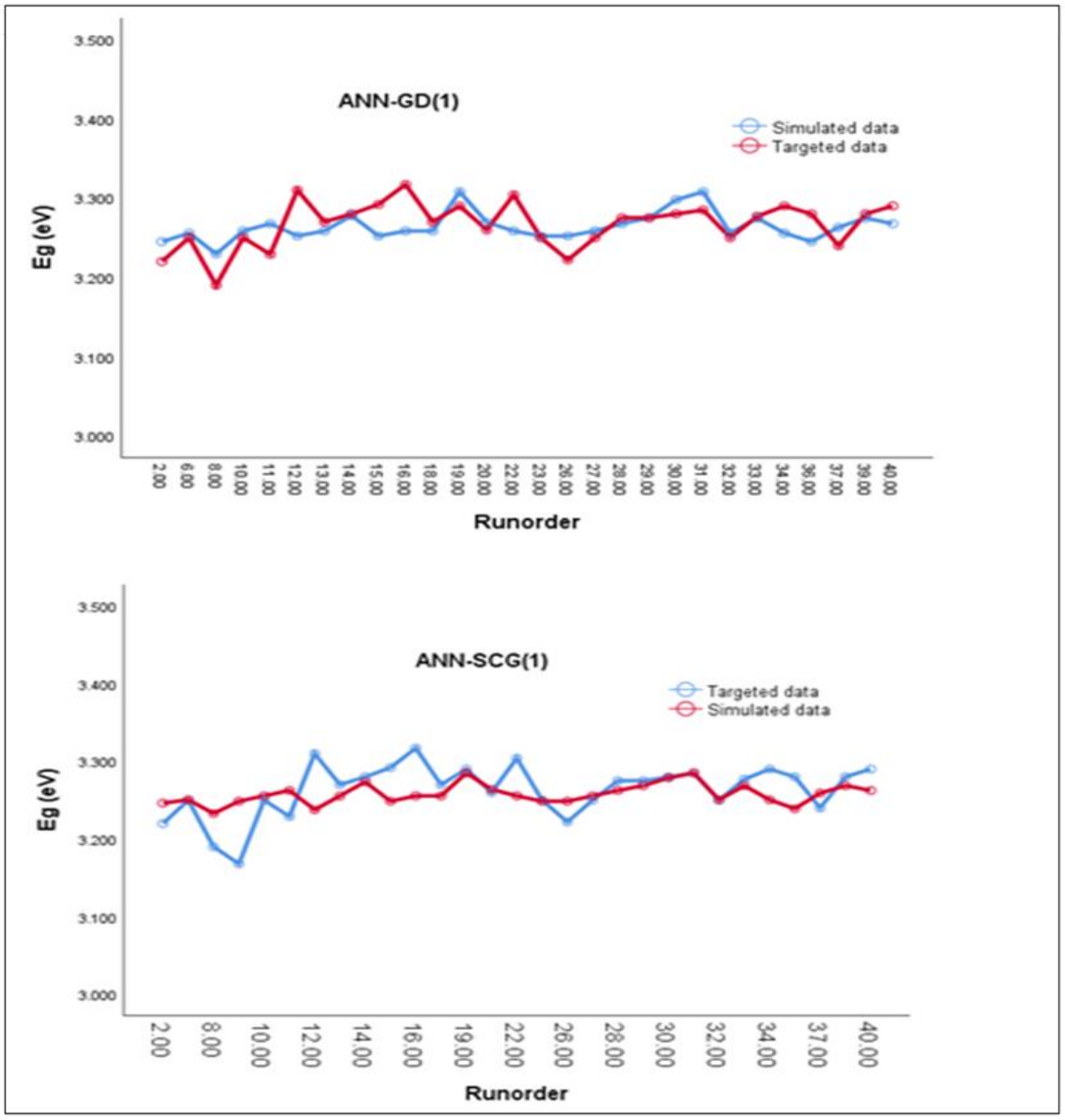

Fig. 4. Simulated and targeted band gap energy of ANN-GD (1) and ANN-SCG (1).

It was observed that the residuals were nearly normally distributed around the line of fit (zero) and no clear patterns or points were found in residuals plots (see Fig. 5). Lastly, in Fig.6, the ANNs models are visualized as three-dimensional surfaces according to the training and testing datasets. It can be observed that the nonlinear correlation between dependant and independent variables presented in the form of non-flat surfaces. ANNs as ML approaches were proven to be potential solution to overcome complexity of nonlinear characteristic between the input and output physical variables.

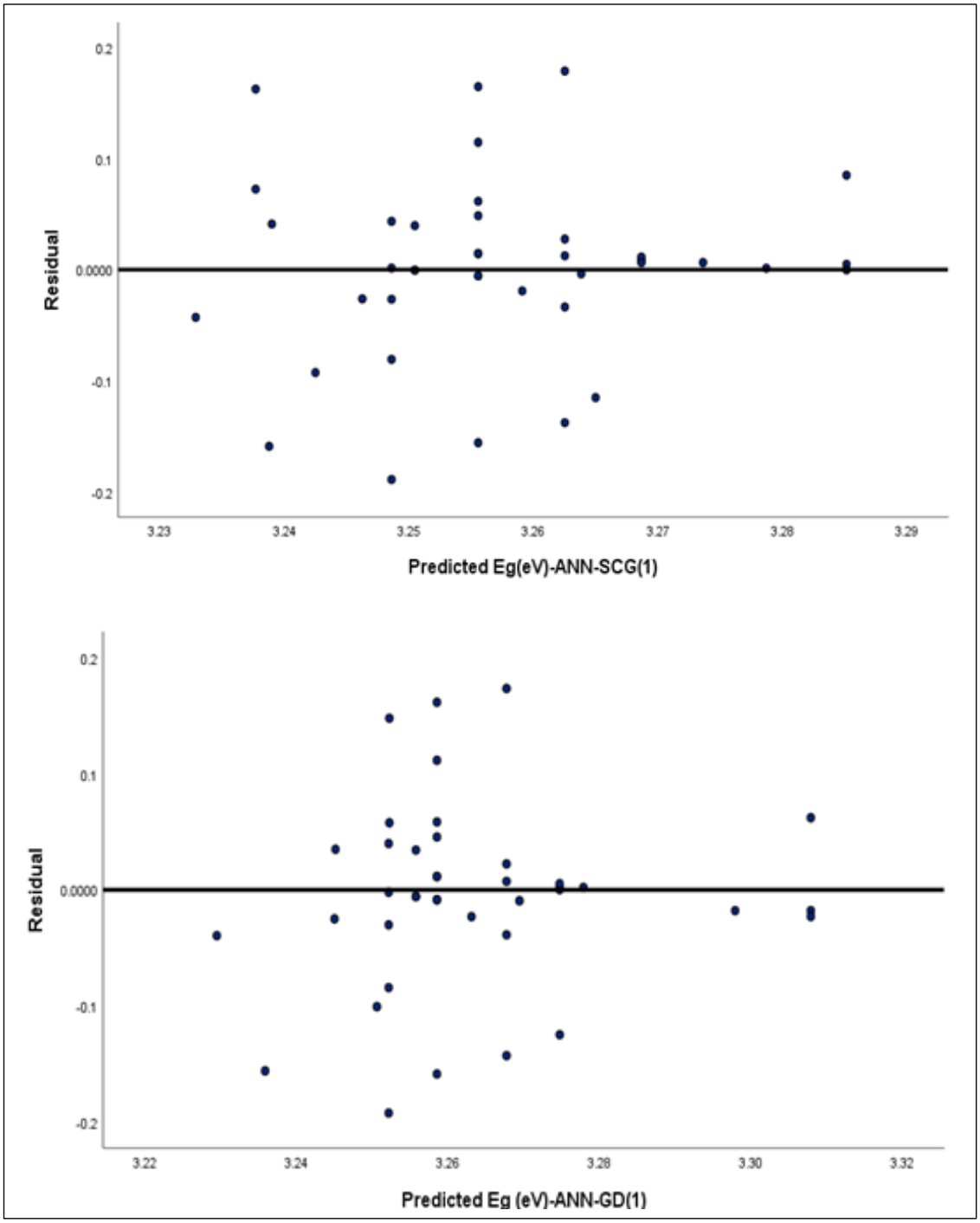

Fig. 5. Residual plots of band gap energy for ANN-GD (1) and ANN-SCG (1).

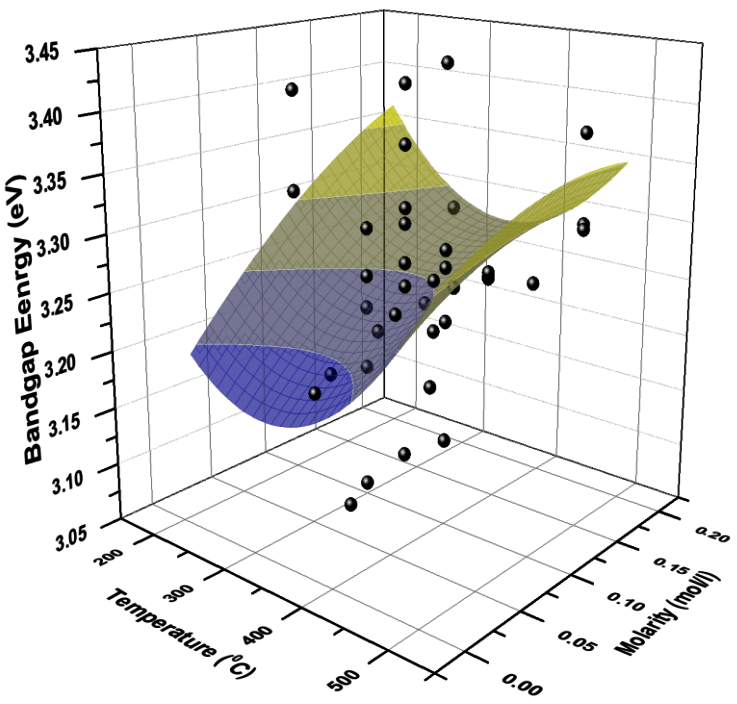

Fig. 6. 3D-surface plot of ANNs model for the band gap energy.

Conclusion

In this study, the comparative predictive ML approaches include ANN-SCG and ANN-GD associated with a conventional MLR technique were investigated to predict the band gap energy of undoped ZnO thin films. The results of ANN-SCG and ANN-GD models showed better performance and significant accuracy with high values of R^2 of 0.9999 and 0.9993, respectively. In contrast, MLR findings had less efficiency with lower value of R^2 of 0.063. In addition, ANN-SCG and ANN-GD showed smaller error in terms of RMSE, MAPE, and r than the MLR analysis. Based on the findings, it was shown that ANNs as ML models were an efficient tool in providing highly predictive accuracy of the system than standard MLR model. Moreover, the obtained results validate that ANNs approach can be adopted for prediction the nonlinear characteristics of nanostructures for highly performed optical devices as well as for comprehensively link the input and output parameters of the fabrication process especially when more factors are taken in consideration.

Abbreviations

Artificial neural networks	ANNs
Scaled conjugate gradient	SCG
Gradient descent	GD
Machine learning	ML
Zinc oxide	ZnO
Photoluminescence	PL
Zinc oxide nanoparticles	ZnO NPs
Adaptive network-based fuzzy inference system	ANFIS
Golden eagle optimizer	GEO
Kernel ridge regression	KRR

Levenberg-Marquardt	LM
Root mean square error	RMSE
Mean absolute percentage error	MAPE

References

[1] Klingshirn, C.F., Waag, A., Hoffmann, A. and Geurts, J., 2010. Zinc oxide: from fundamental properties towards novel applications.

[2] Jagadish, C. and Pearton, S.J. eds., 2011. *Zinc oxide bulk, thin films and nanostructures: processing, properties, and applications*. Elsevier.

[3] Yang, P., Yan, H., Mao, S., Russo, R., Johnson, J., Saykally, R., Morris, N., Pham, J., He, R. and Choi, H.J., 2002. Controlled growth of ZnO nanowires and their optical properties. *Advanced functional materials*, *12*(5), pp.323-331.

[4] Gu, Y., Kuskovsky, I.L., Yin, M., O'Brien, S. and Neumark, G.F., 2004. Quantum confinement in ZnO nanorods. *Applied physics letters*, *85*(17), pp.3833-3835.

[5] Fan, Z., Chang, P.C., Lu, J.G., Walter, E.C., Penner, R.M., Lin, C.H. and Lee, H.P., 2004. Photoluminescence and polarized photodetection of single ZnO nanowires. *Applied physics letters*, *85*(25), pp.6128-6130.

[6] Fan, Z. and Lu, J.G., 2005. Zinc oxide nanostructures: synthesis and properties. *Journal of nanoscience and nanotechnology*, *5*(10), pp.1561-1573.

[7] Liu, Y., Zhao, T., Ju, W. and Shi, S., 2017. Materials discovery and design using machine learning. *Journal of Materiomics*, *3*(3), pp.159-177.

[8] Khude, P., Majumdar, A. and Butola, B.S., 2020. Modelling and prediction of antibacterial activity of knitted fabrics made from silver nanocomposite fibres using soft computing approaches. *Neural Computing and Applications*, *32*, pp.9509-9519.

[9] Amor, N., Noman, M.T., Petru, M. and Sebastian, N., 2022. Comfort evaluation of ZnO coated fabrics by artificial neural network assisted with golden eagle optimizer model. *Scientific Reports*, *12*(1), pp.1-16.

[10] Lu, D. and Yu, W., 2021. Predicting the tensile strength of single wool fibers using artificial neural network and multiple linear regression models based on acoustic emission. *Textile Research Journal*, *91*(5-6), pp.533-542.

[11] Regonia, P.R., Pelicano, C.M., Tani, R., Ishizumi, A., Yanagi, H. and Ikeda, K., 2020. Predicting the band gap of ZnO quantum dots via supervised machine learning models. *Optik*, *207*, p.164469.

[12] Pelicano, C.M., Rapadas, N., Cagatan, G. and Magdaluyo Jr, E., 2017, December. Application of back-propagation artificial neural network (ANN) to predict crystallite size and band gap energy of zno quantum dots. In *AIP conference proceedings* (Vol. 1901, No. 1, p. 020014). AIP Publishing LLC.

[13] Kalantary, S., Jahani, A. and Jahani, R., 2020. MLR and Ann approaches for prediction of synthetic/natural nanofibers diameter in the environmental and medical applications. *Scientific reports*, *10*(1), p.8117.

[14] Benramache, S., Belahssen, O., Guettaf, A. and Arif, A., 2013. Correlation between electrical conductivity—optical band gap energy and precursor molarities ultrasonic spray deposition of ZnO thin films. *Journal of Semiconductors*, *34*(11), p.113001.

[15] Gahtar, A., Benramache, S., Benhaoua, B. and Chabane, F., 2013. Preparation of transparent conducting ZnO: Al films on glass substrates by ultrasonic spray technique. *Journal of Semiconductors*, *34*(7), p.073002.

[16] Bangera, K.V., Anandan, C. and Shivakumar, G.K., 2013. Properties of ZnO: Bi thin films prepared by spray pyrolysis technique. *Journal of alloys and compounds*, *578*, pp.613-619.

[17] Prajapati, C.S., Kushwaha, A. and Sahay, P.P., 2013. Effect of Al dopants on the structural, optical and gas sensing properties of spray-deposited ZnO thin films. *Materials Chemistry and Physics*, *142*(1), pp.276-285.

[18] Chouikh, F., Beggah, Y. and Aida, M.S., 2011. Optical and electrical properties of Bi doped ZnO thin films deposited by ultrasonic spray pyrolysis. *Journal of Materials Science: Materials in Electronics*, *22*, pp.499-505.

[19] Benramache, S. and Benhaoua, B., 2012. Influence of substrate temperature and Cobalt concentration on structural and optical properties of ZnO thin films prepared by Ultrasonic spray technique. *Superlattices and Microstructures*, *52*(4), pp.807-815.

[20] Zhu, B.L., Sun, X.H., Zhao, X.Z., Su, F.H., Li, G.H., Wu, X.G., Wu, J., Wu, R. and Liu, J., 2008. The effects of substrate temperature on the structure and properties of ZnO films prepared by pulsed laser deposition. *Vacuum*, *82*(5), pp.495-500.

[21] Rahal, A., Benramache, S. and Benhaoua, B., 2014. Substrate temperature effect on optical property of ZnO thin films. *Engineering Journal*, *18*(2), pp.81-88.

[22] Benhaoua, B., Rahal, A. and Benramache, S., 2014. The structural, optical and electrical properties of nanocrystalline ZnO: Al thin films. *Superlattices and Microstructures*, *68*, pp.38-47.

[23] Ilican, S., Caglar, Y., Caglar, M. and Demirci, B., 2008. Polycrystalline indium-doped ZnO thin films: preparation and characterization. *Journal of optoelectronics and advanced materials*, *10*(10).
[24] Prajapati, C.S., Kushwaha, A. and Sahay, P.P., 2013. Experimental investigation of spray-deposited Fe-doped ZnO nanoparticle thin films: structural, microstructural, and optical properties. *Journal of thermal spray technology*, *22*, pp.1230-1241.
[25] Hafdallah, A., Ynineb, F., Aida, M.S. and Attaf, N., 2011. In doped ZnO thin films. *Journal of Alloys and Compounds*, *509*(26), pp.7267-7270.
[26] Ilican, S., Caglar, Y., Caglar, M. and Yakuphanoglu, F., 2006. Electrical conductivity, optical and structural properties of indium-doped ZnO nanofiber thin film deposited by spray pyrolysis method. *Physica E: Low-dimensional Systems and Nanostructures*, *35*(1), pp.131-138.
[27] Abed, S., Aida, M.S., Bouchouit, K., Arbaoui, A., Iliopoulos, K. and Sahraoui, B., 2011. Non-linear optical and electrical properties of ZnO doped Ni thin films obtained using spray ultrasonic technique. *Optical Materials*, *33*(6), pp.968-972.
[28] Mosbah, A., Abed, S., Bouhssira, N., Aida, M.S. and Tomasella, E., 2006. Preparation of highly textured surface ZnO thin films. *Materials Science and Engineering: B*, *129*(1-3), pp.144-149.
[29] Zebbar, N., Kheireddine, Y., Mokeddem, K., Hafdallah, A., Kechouane, M. and Aida, M.S., 2011. Structural, optical and electrical properties of n-ZnO/p-Si heterojunction prepared by ultrasonic spray. *Materials Science in Semiconductor Processing*, *14*(3-4), pp.229-234.
[30] Benouis, C.E., Benhaliliba, M., Juarez, A.S., Aida, M.S., Chami, F. and Yakuphanoglu, F., 2010. The effect of indium doping on structural, electrical conductivity, photoconductivity and density of states properties of ZnO films. *Journal of Alloys and Compounds*, *490*(1-2), pp.62-67.
[31] Yakuphanoglu, F., Caglar, Y., Ilican, S. and Caglar, M., 2007. The effects of fluorine on the structural, surface morphology and optical properties of ZnO thin films. *Physica B: Condensed Matter*, *394*(1), pp.86-92.
[32] Roth, A.P., Webb, J.B. and Williams, D.F., 1981. Absorption edge shift in ZnO thin films at high carrier densities. *Solid State Communications*, *39*(12), pp.1269-1271.
[33] Swapna, R., Ashok, M., Muralidharan, G. and Kumar, M.S., 2013. Microstructural, electrical and optical properties of ZnO: Mo thin films with various thickness by spray pyrolysis. *Journal of Analytical and Applied Pyrolysis*, *102*, pp.68-75.
[34] Sadananda Kumar, N., Bangera, K.V. and Shivakumar, G.K., 2014. Effect of annealing on the properties of zinc oxide nanofiber thin films grown by spray pyrolysis technique. *Applied Nanoscience*, *4*, pp.209-216.
[35] Prajapati, C.S., Kushwaha, A. and Sahay, P.P., 2013. Optoelectronics and formaldehyde sensing properties of tin-doped ZnO thin films. *Applied Physics A*, *113*, pp.651-662.
[36] Mhamdi, A., Ouni, B., Amlouk, A., Boubaker, K. and Amlouk, M., 2014. Study of nickel doping effects on structural, electrical and optical properties of sprayed ZnO semiconductor layers. *Journal of alloys and compounds*, *582*, pp.810-822.
[37] Ozutok, F., Demirselcuk, B., Sarica, E., Turkyilmaz, S. and Bilgin, V.İ.L.D.A.N., 2012. Study of ultrasonically sprayed ZnO films: thermal annealing effect. *Acta Physica Polonica A*, *121*(1), pp.53-55.
[38] Aksoy, S., Caglar, Y., Ilican, S. and Caglar, M., 2010. Effect of Sn dopants on the optical and electrical properties of ZnO films. *Optica Applicata*, *40*(1), pp.7-14.
[39] Tokumoto, M.S., Smith, A., Santilli, C.V., Pulcinelli, S.H., Craievich, A.F., Elkaim, E., Traverse, A. and Briois, V., 2002. Structural electrical and optical properties of undoped and indium doped ZnO thin films prepared by the pyrosol process at different temperatures. *Thin solid films*, *416*(1-2), pp.284-293.
[40] Prajapati, C.S., Kushwaha, A. and Sahay, P.P., 2013. Influence of Fe doping on the structural, optical and acetone sensing properties of sprayed ZnO thin films. *Materials Research Bulletin*, *48*(7), pp.2687-2695.